Clinical Pharmacology
in Drug Development
2022, 11(5) 640–653

DOI: 10.1002/cpdd.1070

Pharmacokinetics and Macrophage Inhibitory Cytokine-1 Pharmacodynamics of the Murine Double Minute 2 Inhibitor, Navtemadlin (KRT-232) in Fed and Fasted Healthy Subjects

Shekman Wong[1], Cecile Krejsa[1], Dana Lee[1], Anna Harris[1], Emilie Simard[2], Xiaohui Wang[2], Martine Allard[2], Terry Podoll[3], Terry O'Reilly[4], and J. Greg Slatter[1]

Abstract

This single 60-mg dose, 4-period crossover study assessed the effect of food and formulation change on navtemadlin (KRT-232) pharmacokinetics (PK) and macrophage inhibitory cytokine-1 (MIC-1) pharmacodynamics. Healthy subjects (N = 30) were randomized to 3 treatment sequences, A: new tablet, fasted (reference, dosed twice); B: new tablet, 30 minutes after a high-fat meal (test 1); C: old tablet, fasted (test 2). PK/pharmacodynamic parameters were measured over 0 to 96 hours. Adverse events were mild without any discontinuations. No serious adverse events or deaths occurred. In treatment A, navtemadlin mean (coefficient of variation) maximum concentration (C_{max}) was 525 (66) ng/mL, at median time to maximum concentration (t_{max}) of 2 hours. Mean (coefficient of variation) area under the plasma concentration–time curve from time 0 to time t ($AUC_{0\text{-}t}$) was 3392 (63.3) ng • h/mL, and arithmetic mean terminal half-life was 18.6 hours. Acyl glucuronide metabolite (M1)/navtemadlin $AUC_{0\text{-}t}$ ratio was 0.2, and urine excretion of navtemadlin was negligible. After a meal (B vs A), navtemadlin t_{max} was delayed by 1 hour. Geometric least squares means ratios (90%CI) for navtemadlin C_{max} and $AUC_{0\text{-}t}$ were 102.7% (87.4-120.6) and 81.4% (76.2-86.9), respectively. Old vs new tablet fasted formulations (C vs A) had geometric least squares means ratios (90%CI) of 78.4% (72.0-85.3) for C_{max} and 85.9% (80.5-91.7) for $AUC_{0\text{-}t}$. MIC-1 C_{max} and AUC were comparable across groups; t_{max} was delayed relative to navtemadlin t_{max} by ≈8 hours. Navtemadlin $AUC_{0\text{-}t}$ and MIC-1 $AUC_{0\text{-}t}$ correlated significantly. In conclusion, navtemadlin can be administered safely with or without food; the new formulation does not affect navtemadlin PK. The 60-mg navtemadlin dose elicited a reproducible and robust MIC-1 response that correlated well with navtemadlin exposure, indicating that murine double minute 2 target engagement leads to p53 activation.

Keywords

food effect, GDF15, KRT-232, MDM2 inhibitor, MIC-1, navtemadlin, pharmacodynamics, pharmacokinetics

[1]Kartos Therapeutics, Inc, Redwood City, CA and Bellevue, Washington, USA
[2]Certara Strategic Consulting, Princeton, New Jersey, USA
[3]IV/PO, LLC, Seattle, Washington, USA
[4]Celerion, Tempe, Arizona, USA

Submitted for publication 24 August 2021; accepted 12 December 2021.

Corresponding author:
Shekman Wong, PhD, Kartos Therapeutics, Inc. 275 Shoreline Drive, Suite 300, Redwood City, CA 94065.
e-mail: swong@kartosthera.com

None of the authors is a Fellow of the American College of Clinical Pharmacology (FCP)

Murine double minute 2 (MDM2) is the key negative regulator of the tumor suppressor protein p53. Navtemadlin (KRT-232) is a potent, selective, orally available, small-molecule MDM2 inhibitor that restores p53 activity to drive apoptosis of malignant cells harboring wild-type (WT) *TP53*.[1] Navtemadlin has demonstrated antitumor activity in preclinical xenograft models,[1,2] as well as in patients with solid tumors and multiple myeloma (MM),[3] relapsed/refractory acute myeloid leukemia (AML),[4] Merkel cell carcinoma resistant to anti–programmed cell death protein-1/anti–programmed death ligand-1 inhibitors,[5] and myelofibrosis that has relapsed after or is refractory to Janus-associated kinase inhibitor.[6] Navtemadlin is also being evaluated in a phase 3 trial of patients with relapsed/refractory myelofibrosis,[7] as well as in numerous phase 1b/2 trials in various hematologic malignancies and solid tumors.[8–13]

Macrophage inhibitory cytokine-1 (MIC-1), also known as growth differentiation factor 15 (GDF15), is a secreted pleiotropic member of the transforming growth factor-β family. It is expressed in response to various cellular stressors and modifies pro-growth and pro-apoptosis signal transduction pathways, both in cancer cells and in the tumor microenvironment.[14,15] MIC-1 serum concentration represents a prognostic biomarker in several cancer indications and has recently been implicated in the complex pathogenesis of anorexia and chemotherapy-induced cachexia.[15] MIC-1 is a direct product of p53 transcriptional activation; an increased concentration of serum MIC-1 is a pharmacodynamic (PD) marker of p53-mediated transcriptional activity following MDM2 inhibition in patients treated with navtemadlin.[16]

Navtemadlin is a small-molecule, highly protein-bound (97.5%) monoprotic carboxylic acid (pK_a 4.35) that is primarily metabolized to a major circulating acyl glucuronide metabolite (M1).[17] The structure of navtemadlin and M1 have been previously published.[17–19] In previous studies, M1 has been shown to be stable in vitro and demonstrated 5-fold less pharmacologic activity than the parent drug in a biochemical homogeneous time-resolved fluorescence in vitro pharmacologic potency assay in the presence of 15% serum and was highly bound to plasma proteins.[19] In patients with solid tumors or multiple myeloma, the mean time to maximum concentration (t_{max}) of the metabolite M1 was 2 to 4-hours, and the mean (standard deviation [SD]) terminal half-life ($t_{1/2}$) was 14.0 (6.07) hours. The mean accumulation for metabolite M1 over a 7-day once-daily dosing period was <2-fold, and the mean metabolite-to-parent 24-hour area under the plasma concentration–time curve (AUC) ratio was 0.461. Previously, navtemadlin pharmacokinetics (PK) in patients with cancer were described by a 2-compartment population PK model with first-order absorption using data[20] from 2 oncology studies: a phase 1 study that evaluated navtemadlin in patients with advanced *TP53* WT solid tumors (n = 97) or MM (n = 10),[3] and a phase 1b study that evaluated navtemadlin alone (n = 26) or in combination with trametinib (n = 10) in patients with relapsed or refractory AML.[4] In patients with solid tumors, the median $t_{1/2}$ of navtemadlin was 17.1 hours, the apparent oral central volume of distribution was 62.9 L, and apparent oral clearance (CL/F) was 24.9 L/h. Exposure was linear over a dose range of 15 mg to 480 mg. Overall, PK data in humans was supportive of once-daily dosing.[20] In another study using the same patient population (solid tumors/MM and AML), fixed-effect linear regression modeling indicated that treatment with navtemadlin elicited dose- and plasma concentration–dependent increases in the serum PD marker MIC-1.[16]

Food-drug interactions and formulation changes can have an impact on PK and may alter safety and/or efficacy.[21] Navtemadlin was formulated as an immediate-release, 60-mg, uncoated oral tablet (old tablet) and a new, smaller, film-coated 60-mg tablet with a higher drug load and the same excipients (new tablet). For this reason, we assessed the effect of a high-fat meal and the tablet drug-load change on the PK of navtemadlin and the PD of MIC-1 in healthy subjects. Although increased serum MIC-1 concentrations have been described in patients with cancer treated with a variety of MDM2 inhibitors, this is the first report of PK and MIC-1 PD in healthy subjects. Because *Helicobacter pylori* (*H. pylori*) infection can increase stomach pH[22,23] and might affect navtemadlin dissolution, and because a uridine 5′-diphospho-glucuronosyltransferase (*UGT*) *1A1*28* genotype polymorphism might lead to lower rate of glucuronidation,[24] the effects of these factors on navtemadlin exposure were also assessed.

Methods

Study Design

The study was conducted at Celerion (Tempe, Arizona) based on the principles and requirements of Good Clinical Practice in accordance with the ethical requirements referred to in the European Union directive 2001/20/EC and the Declaration of Helsinki. Written informed consent was obtained from all participants in the study. Before study initiation, all pertinent study documents were reviewed by Advarra Institutional Review Board (Columbia, Maryland).

This single-center, open-label, 60-mg single-dose study consisted of 3 treatments, 4 periods, and 3 sequences. In the initial period (period 1), all healthy subjects received the old tablet under fasted conditions

(treatment C). In Periods 2 through 4, the new tablet was dosed using a 2-treatment, 3-sequence, 3-period crossover partial replicate design, where all subjects received the new tablet twice under fasted conditions and once under fed conditions (Figure S1).

Subjects were randomly assigned to treatment sequences, and the crossover design was used to reduce the residual variability. This partial replicate design reduced the sample size because PK of navtemadlin was highly variable in preliminary oncology studies (ie, intrasubject coefficient of variation [CV] >30%).

The primary objective of the study was to determine the effect of a high-fat meal on the PK of plasma navtemadlin following administration of the new tablet under fed and fasted conditions. Secondary objectives included comparing the PK of plasma navtemadlin following administration of the old tablet to that of the new tablet under fasted conditions, to assess the safety and tolerability of a single 60-mg dose of navtemadlin in healthy subjects, to determine the PK of navtemadlin and navtemadlin acyl glucuronide in plasma, to determine the excretion of navtemadlin and M1 in urine, and to determine the PD of serum MIC-1. Exploratory objectives included monitoring of select immune cell subsets by immunophenotyping, analysis of PK/PD relationship for navtemadlin/MIC-1, and assessing the effect of a high-fat meal on the PD of MIC-1 serum concentrations, and effect of *H. pylori* infection and *UGT1A1*28* genotype on the PK of navtemadlin.

Subjects

Subjects were screened for eligibility up to 28 days before enrollment/first dosing. Subjects with the following eligibility criteria were enrolled: healthy men or women aged 18 to 55 years; health status determined by medical history, physical examination, clinical laboratory tests, vital sign measurements, and 12-lead electrocardiograms performed before the first drug dosing; a body mass index between 18 and 32 kg/m^2; body weight between 50 kg and 100 kg; veins suitable for cannulation or repeated venipuncture; and restraint from strenuous activity or contact sports from 96 hours (4 days) before study entry. Male subjects and female subjects of childbearing or non–childbearing potential, were required to follow reliable methods of contraception as specified by the protocol. Consumption of foods and beverages containing grapefruit/Seville orange was prohibited 14 days before the first dosing and throughout the study (excluding follow-up). Consumption of large amounts of xanthine/caffeine, as well as alcohol, was prohibited 24 hours before the first dosing and throughout the study (excluding follow-up).

Subjects were excluded from the study if they had a clinically significant disorder that interfered with the absorption, distribution, metabolism, or excretion of drugs; creatinine clearance of <80 mL/min based on the Cockcroft-Gault equation; aspartate aminotransferase/alanine aminotransferase and/or total bilirubin above the upper limit of normal at screening; absolute neutrophil count and/or platelets below the lower limit of normal at screening; baseline corrected QT interval by Fridericia > 450 milliseconds for male and > 470 milliseconds for female subjects; had received a live or live-attenuated vaccine in the 2 weeks before the first dose; history of bone marrow transplant or blood transfusion; history of alcohol or drug abuse; and anticipated use of drugs known to be sensitive substrates or significant inducers of cytochrome P450 CYP3A4 and/or CYP2C8 enzymes.

Treatment Groups

All subjects received treatment C: 60 mg navtemadlin (1 × navtemadlin old tablet) under fasted conditions on day 1 of the first study period. After receiving treatment C, subjects were randomly assigned 1:1:1 into 3 groups on day 1 of period 2 to receive the following treatments in a crossover design in periods 2 through 4; treatment A: 60 mg navtemadlin (1 × navtemadlin new tablet) was administered under fasted conditions on 2 occasions per the randomization scheme; treatment B: 60 mg navtemadlin (1 × navtemadlin new tablet) was administered 30 minutes after the start of a high-fat/high-calorie breakfast (Figure S1).

The washout period between single 60-mg navtemadlin doses was 7 days. The washout period of 7 days between doses was >5 navtemadlin half-lives and was considered sufficient to prevent carryover effects of the preceding treatment. Based on the very low rate of adverse events (AEs) reported with 7 consecutive daily doses of navtemadlin (≤120 mg) in patients with cancer (data on file), single 60-mg doses separated by a 1-week washout was deemed safe and well tolerated by healthy subjects. Food effect and drug interaction crossover studies of another MDM2 inhibitor, milademetan, have been conducted using single doses separated by a 1-week washout in healthy subjects.[24]

PK, PD, and safety assessments were performed for 96 hours after each treatment (as described above). Subjects were housed in the clinical research unit on day −1 of period 1 until after the day 5 blood draw and/or study procedures of period 4. All subjects who received at least 1 dose of the study drug returned to the clinical research unit 7 days ± 1 day after the last dose for follow-up procedures and safety assessment. The total study duration from screening through completion of follow-up was ≈8 weeks.

Safety was evaluated by clinical laboratory tests, physical examination, body weight, vital signs, 12-lead electrocardiograms, and AEs. All AEs occurring during

this clinical trial were coded using the Medical Dictionary for Regulatory Activities version 22.1. In the event of an ongoing AE beyond the scheduled follow-up visit, monitoring continued until the AE was resolved or considered stable.

Bioanalytical Methods

Plasma concentrations of navtemadlin and M1 were quantified using stable isotopically labeled internal standards, D_6-navtemadlin and D_6-navtemadlin acyl glucuronide, and the validated liquid chromatography–tandem mass spectrometry method described by Erba et al.[4] Plasma proteins were precipitated with acetonitrile and chromatographed on a Kinetex C_{18} analytical column (2.6 μm, 50 × 3.00 mm; Phenomenex, Torrance, California) with step-gradient elution of 0.1% formic acid in water (mobile phase A [MPA]) and 0.1% formic acid in acetonitrile (mobile phase B) as follows: 0.15 minutes 85% MPA, 0.85 minutes linear gradient to 25% MPA, and holding at these conditions for 0.9 minutes before reequilibrating to 85% MPA at a flow rate of 600 μL/min. Mass spectrometry was conducted using electrospray ionization and negative ion multiple reaction monitoring of parent to product ion pairs *m/z* 566.1→64.1 for navtemadlin, *m/z* 574.3→64.1 for D_6-navtemadlin, *m/z* 742.5→566.0 for navtemadlin acyl glucuronide, and *m/z* 750.4→574.3 for D_6-navtemadlin acyl glucuronide. The lower limit of quantification was 1.00 ng/mL. The interassay precision (%CV) and accuracy (%bias) observed ranged from 4.3 to 6.9 and –5.3 to 3.8 for navtemadlin and 4.7 to 11.7 and –2.2 to 1.1 for navtemadlin acyl glucuronide, respectively.

Urine concentrations of navtemadlin and M1 were quantified using a validated liquid chromatography–tandem mass spectrometry method similar to the plasma method described above, with the following exceptions: human urine samples were treated with isopropanol at a ratio of 20 parts isopropanol to 100 parts urine before being diluted and chromatographed. The interassay precision (%CV) and accuracy (%bias) observed ranged from 1.4 to 4.0 and –1.1 to 3.2 for navtemadlin and 2.1 to 2.6 and –0.3 to 1.7 for navtemadlin acyl glucuronide, respectively.

Serum concentrations of MIC-1 were measured by enzyme-linked immunosorbent assay (GDF-15 Quantikine PDGD150; R&D Systems, Minneapolis, Minnesota); validation of the MIC-1 method at a College of American Pathologists–accredited laboratory demonstrated acceptable analytical accuracy and precision, with limit of quantification at 0.72 pg/mL and verification of dilution linearity to support quantification in high-concentration samples.

Pharmacokinetic Analysis

PK parameters (AUC from time 0 to 24 hours [$AUC_{0\text{-}24}$], AUC from time 0 to time t [$AUC_{0\text{-}t}$], AUC from time 0 to infinity [$AUC_{0\text{-}inf}$], CL/F, C_{max}, t_{max}, and $t_{1/2}$) were calculated using Phoenix WinNonlin version 8.2 (Certara USA, Inc., Princeton, New Jersey). Tables, listings, and figures were generated using Phoenix WinNonlin version 8.2 and third-party reporting tools, including Office Word and Excel 2016 (Microsoft, Redmond, Washington). Statistical analysis for the comparisons between the navtemadlin, navtemadlin acyl glucuronide metabolite (M1), and PK parameter values was performed using SAS version 9.4 (SAS Institute, Cary, North Carolina).

Blood samples for measurement of plasma concentrations of navtemadlin and M1 metabolite were collected during each period: before dosing (0 hours) and at 0.5, 1, 1.5, 2, 3, 4, 6, 8, 10, 12, 24, 36, 48, 72, and 96 hours after navtemadlin administration. Urine samples for PK assessment of navtemadlin and M1 were collected only in period 1 before dosing (spot collection) and for pooled intervals as follows: 0 to 4, 4 to 8, 8 to 12, 12 to 24, and 24 to 48 hours after navtemadlin administration. Concentration values of navtemadlin and M1 in plasma and urine that were reported as below the limit of quantitation (BLQ) were set to 0 for PK parameter calculation and concentration summary statistics. The urinary PK parameters for urine were reported as total amount of parent drug or M1 excreted unchanged in urine; calculated as Ae = Σ(concentration * volume), molar fraction (in %) of parent drug or M1 excreted unchanged in urine relative to dose calculated as fe = 100*Ae/dose, and renal clearance of parent drug calculated as Ae (parent)/$AUC_{0\text{-}inf\ plasma}$ (parent).

Plasma PK parameter calculations for each study period were performed using actual times calculated relative to the time of study drug administration in hours. Navtemadlin and M1 amounts and fraction excreted in urine were calculated over the separate and combined collection intervals.

Pharmacodynamic Analysis

Key PD parameters analyzed were $AUC_{0\text{-}24}$, $AUC_{0\text{-}t}$, and $AUC_{0\text{-}inf}$, C_{max}, fold change in concentration from predose (baseline: P) at C_{max} ($Fold_{Cmax}$), t_{max}, $t_{1/2}$, baseline concentration, and percent change from predose (baseline: P) concentration at C_{max} ($\%CFB_{Cmax}$). Blood samples for measurement of serum concentrations of MIC-1 were collected at each period: before dosing (0 hours) and at 1, 2, 4, 8, 12, 24, 36, 48, 72, and 96 hours after navtemadlin administration. Serum PD parameter calculations were performed using actual times calculated relative to the time of study drug administration in hours. PD parameters were determined based on individual serum concentration–time data for MIC-1. Concentration values of serum MIC-1 that are reported as BLQ were set to 0 for PD parameter calculation and concentration summary statistics, except for

calculation of %CFB at 24 hours after dosing (%$CFBC_{24}$), %CFB_{Cmax}, $Fold_{C24}$, and $Fold_{Cmax}$, where BLQ values were replaced by the MIC-1 lower limit of quantitation (24 pg/mL).

PK (in plasma) and PD (MIC-1 in serum) parameters were summarized with the following descriptive statistics: n, mean, SD, %CV, median, minimum, maximum, arithmetic mean, and geometric mean %CV. Half-life of navtemadlin was calculated as arithmetic mean ± SD. A correlation analysis of plasma navtemadlin $AUC_{0\text{-}t}$ (PK) vs serum MIC-1 $AUC_{0\text{-}t}$ (PD) was also performed using molar equivalent AUCs (nM * h).

Additional Analyses

An *H. pylori* breath test was performed by Quest Diagnostics (Chantilly, Virginia) on day –1 of period 1 for each subject.

Genotyping for *UGT1A1*28* polymorphisms, (**1*1* [6/6 TA repeats], **1*28* [6/7 TA repeats], and **28*28* [7/7 TA repeats]) was performed by Interpace Pharma Solutions (formerly CGI; Morrisville, North Carolina) on a blood sample taken before dosing on day 1 of period 1. For immunophenotyping, whole blood samples were collected at the screening visit, during periods 1 and 4 (only) on day 1 before dosing, and on day 5 (96 hours) after dosing for each subject. Flow cytometry was performed by Celerion Bioanalytical (Lincoln, Nebraska). A validated, good laboratory practice–compliant method was used to determine the absolute counts and percentages of T, B, and natural killer lymphocytes in peripheral blood (dipotassium ethylenediaminetetraacetic acid) samples.

Sample Size and Statistical Analysis

Assuming an intrasubject %CV of 37% based on PK of the old tablet in patients with cancer, a 95% relative change in exposure under test conditions (fed/fasted) and 90%CIs for the geometric mean ratios (GMRs) for AUC and C_{max}, 24 subjects were required to achieve 80% power. Allowing for 20% dropouts, 30 subjects were planned to ensure ≈24 evaluable subjects.

Because the intrasubject variability of the PK parameters of the reference formulation (new tablets under fasted condition) was not high (ie, <30%), the reference-scaled average bioequivalence approach was not necessary, and the standard linear mixed-effects modeling approach was used to compute the GMRs of the PK parameters AUC and C_{max} and respective 90%CIs to determine food effect and formulation effects. The target range for comparability of food and formulation was when the 90%CI was within the range of 80% to 125% for C_{max} and $AUC_{0\text{-}t}$. Food-effect studies of drug candidates in early clinical development are not usually powered to meet formal bioequivalence standards, and differences in exposure were considered relative to overall population PK–derived variability in navtemadlin CL/F (>50%) in decisions regarding administration with food and the adoption of the new tablet formulation. Comparison of t_{max} was performed nonparametrically using the Wilcoxon signed-rank test. A mixed-effects model approach was used to assess the relative bioavailability using GMRs for $AUC_{0\text{-}24}$, $AUC_{0\text{-}t}$, $AUC_{0\text{-}inf}$, and C_{max} of navtemadlin.

Results

Demographics

A total of 30 healthy subjects were enrolled in the study and were randomly assigned to 1 of the 3 treatment sequences (n = 10 for each treatment sequence); all 30 subjects completed the study. The proportion of men was higher than women (57% vs 43%), with 93% White and 7% Black or African American subjects. Overall, 77% subjects of the overall population were Hispanic or Latino. The median age was 39.5 years (range, 18-54). The mean weight (SD) was 74.5 kg (8.8), and the mean height (SD) was 166.5 cm (8.5), with a mean body mass index (SD) of 26.9 kg/m^2 (2.6). Subject demographics were balanced among the 3 treatment sequence groups (Table S1).

Safety

All 30 subjects received navtemadlin per protocol and were included in the safety analysis. No deaths or serious AEs occurred during the study, and no subject discontinued due to an AE. Nine subjects experienced treatment-emergent adverse events (TEAEs) with treatment C (old formulation, fasted state), 5 subjects experienced TEAEs with treatment A (new formulation in fasted state), and 2 subjects experienced TEAEs with treatment B (new formulation in fed state). Headache was the only TEAE related to navtemadlin reported once for the new formulation (fed state) treatment B.

The most frequently reported TEAE in this study was constipation (13%), which occurred only with treatment C (old formulation, fasted state), followed by headache (10%), which occurred with all treatments A, B, and C. The incidence of TEAEs was highest at 30% during the first period of the study, which was treatment C (old tablet fasted) for all subjects. The overall incidence of TEAEs decreased and was similar (7%-10%) following the remaining treatments (first and second administration of treatment A: new tablet fasted and treatment B: new tablet fed) (Table S2).

Immunophenotyping

Because navtemadlin is being developed for the treatment of myeloproliferative disorders, immunophenotyping of whole blood samples collected at screening,

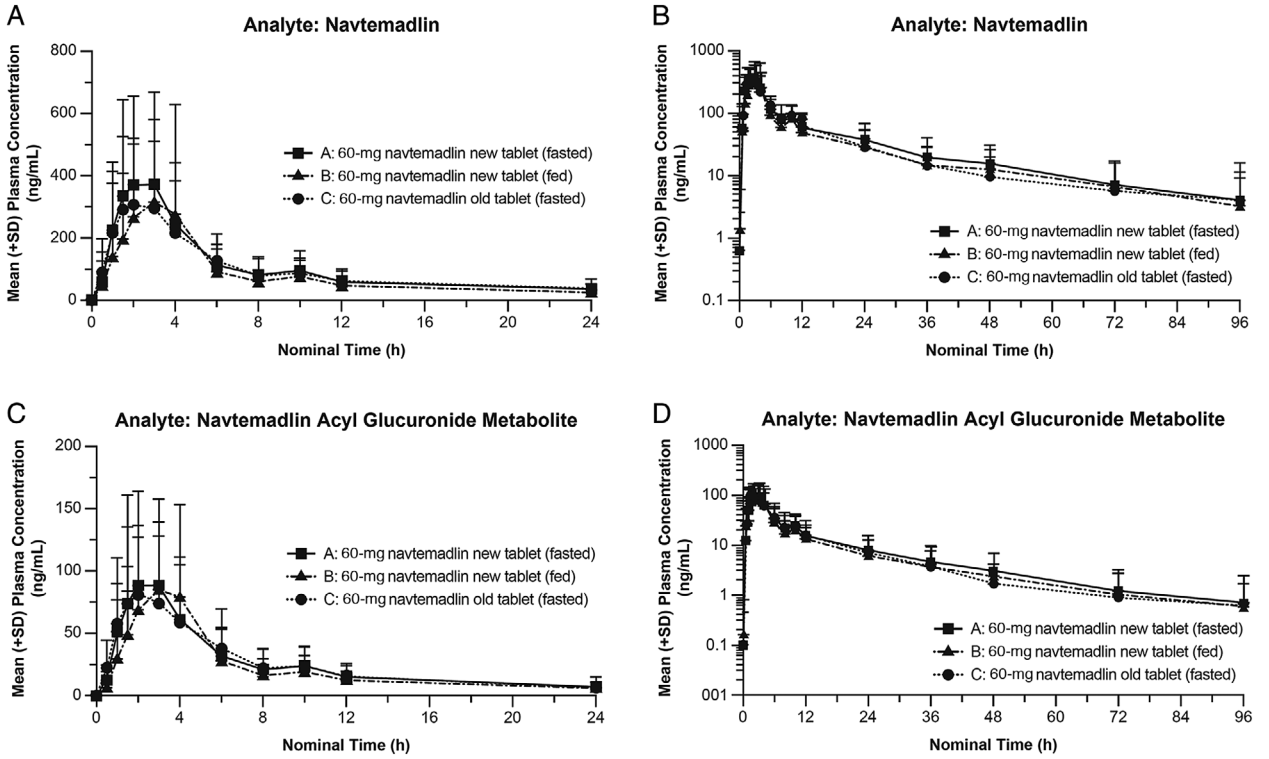

Figure 1. Mean (+SD) plasma concentrations of 60-mg navtemadlin over 24 hours on a linear scale (A) and over 96 hours on a semilog scale (B), and of acyl glucuronide metabolite (M1) over 24 hours on a linear scale (C) and over 96 hours on a semilog scale (D). SD, standard deviation.

before dosing, and 96 hours after dosing (periods 1 and 4) was undertaken to monitor potential effects on peripheral blood lymphocytes and monocytes in healthy subjects. Lymphocyte subsets, as absolute counts per microliter of blood, and as percentages of T, B, and natural killer cells within the CD45+ gate; and monocytes, as percentages of CD14+ cells within the CD45+ gate, did not differ in the postdose samples (96 hours) from predose samples. All changes in absolute counts or percentages were within normal fluctuations during the predose period (data not shown). As no changes to immune subsets were observed, subgroup analysis changes under fasted vs fed conditions was not performed.

Pharmacokinetic Parameters of Navtemadlin and M1 in Plasma and Urine

Mean (SD) concentration-time plots of navtemadlin and M1 for the 30 enrolled subjects are shown in Figure 1A and B (navtemadlin) and Figure 1C and D (M1), respectively. For treatment A, the mean of 2 replicated PK measurements was determined. As a result, this group had twice the number of observations relative to treatments B and C. Most of the subjects had measurable plasma concentrations of navtemadlin up to 96 hours after dosing for all 3 treatments. Only a few subjects showed measurable concentrations of M1 up to 96 hours after dosing. For both navtemadlin and M1, mean peak plasma concentration was observed between 2 and 4 hours, followed by a second peak around 10 hours after dosing that is likely to be a result of enterohepatic recirculation (EHR) of navtemadlin. Detailed PK parameters of navtemadlin and M1 are shown in Table 1.

Following a single administration of the new navtemadlin 60-mg tablet, dosed on 2 separate occasions to each subject under fasted conditions (treatment A), median navtemadlin t_{max} was at 2 hours after dosing. Mean $AUC_{0\text{-}24}$ was 2492 ng • h/mL (55 %CV), and mean C_{max} was 525 ng/mL (66 %CV). The terminal phase for navtemadlin was well characterized with a low extrapolated AUC, and the arithmetic mean half-life was 18.6 hours. CL/F for navtemadlin was 23.7 L/h. The median navtemadlin acyl glucuronide metabolite (M1) t_{max} was 2.02 hours after dosing. Mean $AUC_{0\text{-}24}$ was 607 (60.9 %CV) ng • h/mL, mean C_{max} was 118 ng/mL (70 %CV), and the arithmetic mean half-life was 16.2 hours. After correction for molecular weight, the acyl glucuronide to parent drug $AUC_{0\text{-}t}$ ratios were consistent across study groups at ≈0.2.

The mean navtemadlin amount and fraction of dose excreted in urine were 12.1 μg and 0.02%, respectively. The mean renal clearance for navtemadlin was ≈4.6 mL/h (or 0.0046 L/h). Mean navtemadlin acyl

Table 1. Mean (CV%) Plasma Pharmacokinetic Parameters of Navtemadlin and Its Acyl Glucuronide Metabolite Following Administration of 60-mg Navtemadlin New Tablet (Treatment A[a]), Old Tablet (Treatment C) Under Fasted Conditions, and the New Tablet Under Fed Conditions (Treatment B)

Parameter	A: 60-mg Navtemadlin (New Tablet) Fasted N = 30[a]	B: 60-mg Navtemadlin (New Tablet) Fed N = 30	C: 60-mg Navtemadlin (Old Tablet) Fasted N = 30
		Mean (%CV); n	
Navtemadlin			
$AUC_{0\text{-}24}$, ng • h/mL	2492 (55.0); 60	2027 (54.5); 30	2308 (57.5); 30
$AUC_{0\text{-}t}$, ng • h/mL	3392 (63.3); 60	2752 (66.9); 30	2984 (68.3); 30
$AUC_{0\text{-}inf}$, ng • h/mL	3430 (64.4); 55	2926 (75.0); 27	2870 (61.1); 28
C_{24}, ng/mL	37.4 (83.9); 60	29.3 (83.3); 30	29.3 (83.6); 30
C_{max}, ng/mL	525 (66.0); 60	544 (71.7); 30	410 (67.8); 30
t_{max},[b] h	2.00 (0.67 – 6.00); 60	3.00 (0.99 – 4.02); 30	2.01 (1.00 – 6.00); 30
CL/F, L/h	23.7 (50.6); 55	29.3 (55.6); 27	29.1 (56.0); 28
$t_{1/2}$,[c] h	18.6 (41.6); 55	18.8 (50.9); 27	19.6 (57.4); 28
Acyl Glucuronide Metabolite (M1)			
$AUC_{0\text{-}24}$, ng • h/mL	607 (60.9); 60	532 (56.0); 30	609 (68.6); 30
$AUC_{0\text{-}t}$, ng • h/mL	782 (72.2); 60	666 (65.8); 30	740 (77.5); 30
$AUC_{0\text{-}inf}$, ng • h/mL	849 (74.1); 46	824 (61.1); 22	794 (71.6); 26
C_{24}, ng/mL	7.82 (97.4); 60	5.96 (87.8); 30	7.04 (109.6); 30
C_{max}, ng/mL	118 (70.0); 60	133 (52.6); 30	101 (65.3); 30
t_{max},[b] h	2.02 (1.00 – 6.00); 60	3.00 (0.99 - 4.02); 30	2.01 (1.00 – 6.00); 30
$t_{1/2}$,[c] h	16.2 (57.8); 46	19.6 (61.0); 22	13.7 (68.5); 26
M/P ($AUC_{0\text{-}t}$)	0.2 (32.9); 60	0.2 (38.3); 30	0.2 (34.3); 30

AUC_{inf}, area under the plasma concentration–time curve from time 0 to infinity; $AUC_{0\text{-}24}$, area under the plasma concentration–time curve from time 0 to 24 hours; $AUC_{0\text{-}t}$, area under the plasma concentration–time curve from time 0 to time t; CL/F, apparent oral clearance; C_{max}, maximum observed plasma concentration; CV, coefficient of variation; M/P, metabolite-to-parent ratio; $t_{1/2}$, terminal elimination half-life; t_{max}, time to C_{max}.
[a] Treatment A only: mean of 2 separate PK parameter determinations = treatment A was administered on 2 occasions.
[b] Median (min-max); n.
[c] Arithmetic mean (%CV).
N = number of subjects per group, n = number of observations.

glucuronide metabolite amount and fraction of dose excreted in urine were 17.3 µg and 0.02%, respectively.

Effect of Food

Following administration of the new tablet with a high-fat meal, the percent ratios of geometric least squares means (GLSM) (90%CI) for $AUC_{0\text{-}24}$ were 82.2 (77.2-87.5) for navtemadlin and 88.2 (82.2-94.6) for M1. Overall, the GLSM ratios for AUC were within the 80% to 125% bioequivalence limits for navtemadlin; however, the lower end of the 90%CIs fell slightly below 80% (Table 2). For C_{max}, no difference was observed for the new tablet in fed and fasted states for navtemadlin (GLSM [90%CI]: 102.7 [87.4-120.6]), whereas an increase of ≈18% was observed for M1 following administration of the new tablet with a high-fat meal (GLSM [90%CI]: 118.7 [105.4-133.6]). The difference in median t_{max} between the fed and fasted conditions (new tablet) was statistically significant for navtemadlin but was not significant for M1 (at alpha level of 0.1). Overall, a high-fat meal generally decreased the extent of exposure ($AUC_{0\text{-}24}$, $AUC_{0\text{-}t,}$ and $AUC_{0\text{-}inf}$) to navtemadlin and M1 by ≈12% to 18% following administration of the new tablet. The rate of absorption (C_{max}) after a high-fat meal did not differ markedly for navtemadlin but was ≈20% higher for M1. These were deemed to be small differences in exposure, relative to overall population PK–derived variability in navtemadlin clearance observed in patients with cancer (62 %CV).[20] As such, navtemadlin can be administered with or without food.

Effect of Change in Navtemadlin Tablet Drug Load

With the old tablet administered under fasted conditions, relative to the new tablet administered under fasted conditions, slight decreases were noted in navtemadlin $AUC_{0\text{-}24}$ (2180 vs 1976 ng • h/mL), with a percent ratio of GLSM (90%CI) of 90.7 (85.6-96.0). A small decrease was observed for M1 $AUC_{0\text{-}24}$ (528 vs 506 ng • h/mL), with percent ratio of GLSM (90%CI) of 95.8 (89.4-102.7) (Table 3). The 90%CI for the ratio of GLSM between old and new formulations for all AUCs of both analytes fell within the equivalence limits of 80% to 125%CI, except for navtemadlin $AUC_{0\text{-}inf}$ (GLSM [90%CI]: 79.0-90.6). The C_{max} GLSM ratios

Table 2. GLSM Ratios and 90%CIs of Navtemadlin and Its Acyl Glucuronide Metabolite Following Administration of 60-mg Navtemadlin New Tablet Under Fed Conditions (Treatment B) vs Fasted Conditions (Treatment A[a]) (Food Effect)

PK Parameters	60-mg Navtemadlin New Tablet Fed Treatment B (Test 1)[a]	60-mg Navtemadlin New Tablet Fasted[b] Treatment A (Reference)[a]	% Ratio of Least Squares Means 90%CI (Lower, Upper) (Test/Reference)[c]
Navtemadlin			
$AUC_{0\text{-}inf}$, ng • h/mL	2443, N = 27	2987, N = 30[c]	81.8 (76.0-88.1)
$AUC_{0\text{-}24}$, ng • h/mL	1791, N = 30	2180, N = 30	82.2 (77.2-87.5)
$AUC_{0\text{-}t}$, ng • h/mL	2325, N = 30	2858, N = 30	81.4 (76.2-86.9)
C_{max}, ng/mL	442, N = 30	431, N = 30	102.7 (87.4-120.6)
t_{max}, h	3.0[d]	2.1[d]	0.5 (0.004-0.9)[e,f]
Acyl Glucuronide Metabolite (M1)			
$AUC_{0\text{-}inf}$, ng • h/mL	610, N = 22	710, N = 28	86.0 (77.5-95.4)
$AUC_{0\text{-}24}$, ng • h/mL	465, N = 30	528, N = 30	88.2 (82.2-94.6)
$AUC_{0\text{-}t}$, ng • h/mL	555, N = 30	646, N = 30	85.9 (79.9-92.3)
C_{max}, ng/mL	117, N = 30	98, N = 30	118.7 (105.4-133.6)
t_{max}, h	3.0[d]	2.5[d]	0.4 (-0.002-0.8)[e,g]

AUC_{inf}, area under the plasma concentration–time curve from time 0 to infinity; $AUC_{0\text{-}24}$, area under the plasma concentration-time curve from time 0 to 24 hours; $AUC_{0\text{-}t}$, area under the plasma concentration–time curve from time 0 to time t; C_{max}, maximum observed plasma concentration; CV, coefficient of variation; GLSM, geometric least squares mean; PK, pharmacokinetic; $t_{1/2}$, terminal elimination half-life; t_{max}, time to C_{max}.
[a] GLSM, N; where N is the number of subjects who are included in the analysis. GLSMs are the least square means from analysis of variance presented following back transformation to the original scale.
[b] Treatment A only: mean of 2 separate PK parameter determinations = treatment A was administered on 2 occasions.
[c] The 90%CIs are presented following back transformation to the original scale.
[d] N = 30; N is the number of subjects who had results of both test and reference drugs, and the reference t_{max} is the average of 2.
[e] Difference of medians 90%CI (lower, upper) (test-reference).
[f] *P* value (Wilcoxon signed-rank test) = 0.098.
[g] *P* value (Wilcoxon signed-rank test) = 0.112.

(90%CI) were 78.4 (72.0-85.3) and 85.7 (77.9-94.2) for navtemadlin and M1, respectively; therefore, the GLSM ratios for navtemadlin did not fall within formal equivalence limits of 80% to 125%CI (Table 3). The difference in median t_{max} was not statistically significant ($P > .05$). Overall, the extent of exposure (AUC) to navtemadlin and M1 was similar for the old and new tablets under fasted conditions, whereas the rate of absorption (C_{max}) was generally lower for the navtemadlin old 60-mg tablet. These were deemed to be small differences in exposure, relative to overall population PK–derived variability in navtemadlin clearance observed in cancer patients (62 %CV).[20] As such, the change in tablet drug load did not affect PK of navtemadlin.

H. pylori *Assessment*

The PK of navtemadlin was not markedly different in *H. pylori*–positive subjects (n = 12) compared with *H. pylori*–negative subjects (n = 18), indicating that higher gastric pH, a common characteristic of *H. pylori*–positive subjects,[23,25] does not markedly alter the rate and extent of navtemadlin exposure. Box plots for the treatment A group are presented in Figure 2. The box plots showed similar mean values for $AUC_{0\text{-}24}$ and C_{max} by *H. pylori* status with substantial overlap in PK distribution, demonstrating the similarity of exposures relative to *H. pylori* status.

UGT1A1*28 *Genotyping*

Navtemadlin exposure in *UGT1A1*28* heterozygous poor metabolizers (6/7 thymine-adenine [TA] repeats) was slightly lower than *UGT1A1*28* WT subjects (6/6 TA repeats), suggesting that UGT1A1 is not likely to be rate limiting in navtemadlin clearance. Box plots comparing $AUC_{0\text{-}24}$ and C_{max} among the different observed genotypes are presented in Figure S2. The comparison of other genotypes of *UGT1A1*28* (5/6 and 7/7 TA repeats) vs *UGT1A1*28* WT (6/6 TA repeats) could not be performed due to lack of a sufficient number of observations.

Pharmacodynamic Parameters of MIC-1 in Serum

The mean (SD) concentration-time plots of MIC-1 following all 3 treatments are shown in Figure 3 and PD parameters for MIC-1 are summarized in Table 4. The mean MIC-1 AUC and baseline concentration, $C_{max,}$ and C_{24} values of MIC-1 were generally comparable after administration of the new tablet under fed and fasting conditions. Ratios of the mean MIC-1 $AUC_{0\text{-}t}$ and C_{max} from fed vs fasted for the new tablet ranged between 0.86 and 0.91, consistent with the navtemadlin

Table 3. GLSM Ratios and 90%CIs of Navtemadlin and Its Acyl Glucuronide Metabolite Following Administration of 60-mg Navtemadlin Old Tablet (Treatment C) vs New Tablet Under Fasted Conditions (Treatment A[a]) (Effect of Drug Load Change)

PK Parameters	60-mg Navtemadlin Old Tablet Fasted Treatment C (Test 2)[a]	60-mg Navtemadlin New Tablet Fasted[b] Treatment A (Reference)[a]	% Ratio of Least Squares Means 90%CI (Lower, Upper) (Test/Reference)[c]
Navtemadlin			
$AUC_{0\text{-}inf}$, ng • h/mL	2519, N = 28	2978, N = 30	84.6 (79.0 to 90.6)
$AUC_{0\text{-}24}$, ng • h/mL	1976, N = 30	2180, N = 30	90.7 (85.6 to 96.0)
$AUC_{0\text{-}t}$, ng • h/mL	2455, N = 30	2858, N = 30	85.9 (80.5 to 91.7)
C_{max}, ng/mL	337, N = 30	431, N = 30	78.4 (72.0 to 85.3)
t_{max}, h	2.0[d]	2.1[d]	0.1 (–0.3 to 0.6)[e,f]
Acyl Glucuronide Metabolite (M1)			
$AUC_{0\text{-}inf}$, ng • h/mL	643, N = 26	701, N = 28	91.8 (85.3 to 98.6)
$AUC_{0\text{-}24}$, ng • h/mL	506, N = 30	528, N = 30	95.8 (89.4 to 102.7)
$AUC_{0\text{-}t}$, ng • h/mL	585, N = 30	646, N = 30	90.6 (84.2 to 97.6)
C_{max}, ng/mL	84, N = 30	98, N = 30	85.7 (77.9 to 94.2)
t_{max}, h	2.0[d]	2.5[d]	0.1 (–0.3 to 0.6)[e,g]

AUC_{inf}, area under the plasma concentration–time curve from time 0 to infinity; $AUC_{0\text{-}24}$, area under the plasma concentration–time curve from time 0 to 24 hours; $AUC_{0\text{-}t}$, area under the plasma concentration–time curve from time 0 to time t; C_{max}, maximum observed plasma concentration; CV, coefficient of variation; GLSM, geometric least squares mean; PK, pharmacokinetic; $t_{1/2}$, terminal elimination half-life; t_{max}, time to C_{max}.

[a] GLSM, N; where N is the number of subjects who are included in the analysis. GLSMs are the least square means from analysis of variance presented following back transformation to the original scale.

[b] Treatment A only: mean of 2 separate PK parameter determinations = treatment A was administered on 2 occasions.

[c] The 90%CIs are presented following back transformation to the original scale.

[d] N = 30, N is the number of subjects who had results of both test and reference drugs and the reference t_{max} is the average of 2.

[e] Difference of medians 90%CI (lower, upper) (test-reference).

[f] *P* value (Wilcoxon signed-rank test) = .567.

[g] *P* value (Wilcoxon signed-rank test) = .741.

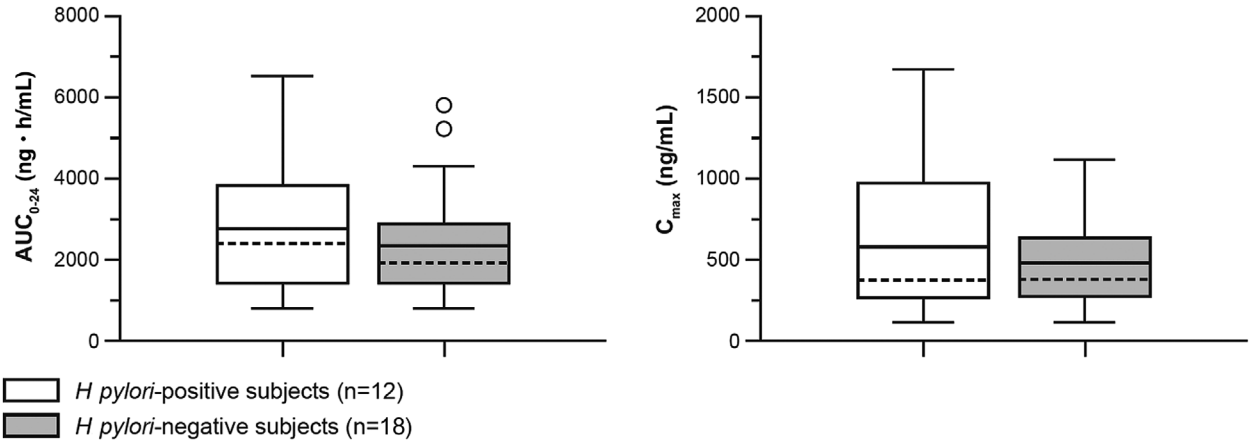

Figure 2. Box plot of navtemadlin PK parameters $AUC_{0\text{-}24}$ and C_{max} by *H. pylori* status following administration of 60-mg navtemadlin new tablet under fasted conditions (treatment A)[a]. $AUC_{0\text{-}24}$, area under the plasma concentration–time curve from time 0 to 24 hours.

[a] For Treatment A, the mean of 2 replicated PK measurements was counted.

Values from both periods when the navtemadlin new tablet was administered under fasting conditions are included. The dashed line corresponds to the median; the solid line to the arithmetic mean. The ends of the "box" are the 25th and 75th percentiles, also referred to as the first and third quartiles. The whiskers show the lowest data value still within 1.5 IQR of the lower quartile, and the highest value still within 1.5 IQR of the upper quartile, where IQR is the interquartile range (the difference between the third and first quartiles, the middle 50%). Data values that do not fall between the whiskers are plotted as outliers (markers outside of the whiskers).

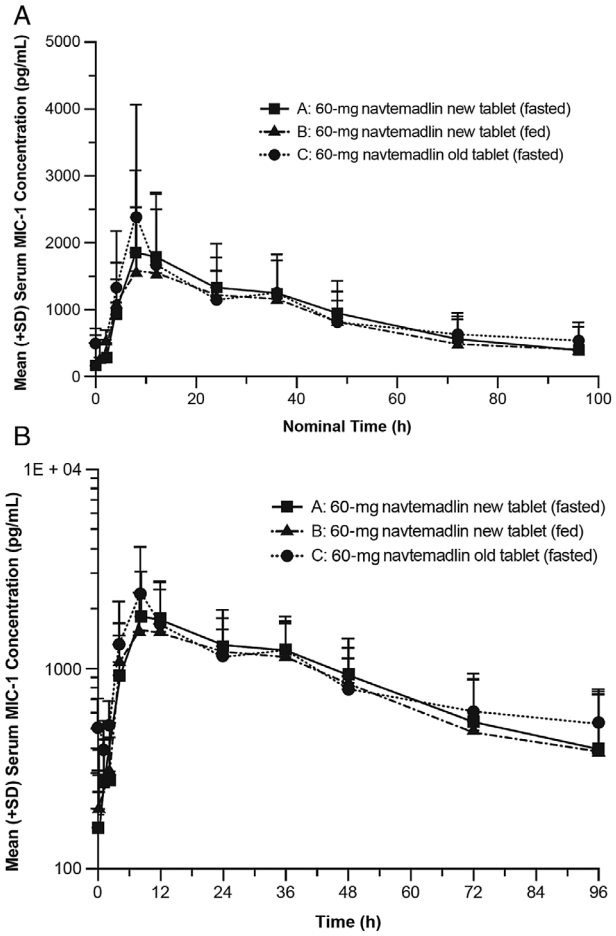

Figure 3. Mean (+SD) serum concentrations of MIC-1 over 96 hours following administration of 60-mg navtemadlin in (A) linear and (B) semilogarithmic format showing comparable concentration versus time profile among subject groups receiving treatment A, B, or C. MIC-1, macrophage inhibitory cytokine-1; SD, standard deviation.

PK results above. The median t_{max} for MIC-1 under new tablet fasted-state conditions was observed at 12.01 hours after dosing.

The mean MIC-1 AUC, C_{max}, and C_{24} for the old tablet administered in the fasted state were comparable to that of the new tablet fasted state. Notably, however, mean initial baseline MIC-1 concentration was slightly higher for the old tablet fasted condition (505 pg/mL), compared with the new tablet under fed and fasted conditions (214 and 170 pg/mL, respectively; Table 4). This may be related to a period effect because the fasted old tablet cohort was dosed in period 1, and the other results were obtained 1 week after a prior navtemadlin dose.

Pharmacokinetic/Pharmacodynamic Relationship

The 60-mg navtemadlin dose elicited a robust and navtemadlin plasma concentration–dependent PD response in serum MIC-1. All 3 treatments resulted in generally comparable MIC-1 AUC and C_{max}, indicating that the tablet drug load or fed vs fasted administration did not meaningfully affect navtemadlin PD. Figure 4A demonstrates the significant correlation observed between navtemadlin $AUC_{0\text{-}t}$ and MIC-1 $AUC_{0\text{-}t}$ in subjects receiving treatment A ($R^2 = 0.68$; intercept, 1.97; slope = 0.0006), and Figure 4B illustrates the pronounced hysteresis that is observed due to the 8- to 12-hour delay in MIC-1 t_{max}, relative to navtemadlin t_{max}. This delayed action is consistent with induction of MIC-1 gene expression and protein synthesis, following reactivation of p53 by navtemadlin.

Discussion

In this study, we characterized the effect of a high-fat meal and a tablet drug load change on the PK, PD, and safety of navtemadlin and its acyl glucuronide metabolite (M1) in healthy subjects.

The magnitude of the food effect was relatively small; therefore, a dose adjustment is not warranted when navtemadlin is administered with food. Similarly, small differences in C_{max} and $AUC_{0\text{-}t}$, relative to overall PK variability, indicated that the old and new tablet formulations are interchangeable.

Navtemadlin PK parameters for the old tablet dosed in healthy subjects under fasted conditions compared favorably with PK data derived from patients with cancer receiving this formulation under fasted conditions.[20] The CL/F of 29.1 L/h observed in healthy subjects in the current study after administration of the old tablet under fasted conditions compared well to navtemadlin median CL/F of 24.9 L/h in the solid tumor population under fasted conditions. The model-derived terminal half-life in patients with solid tumors was 17 hours, which was the same as that observed for the new tablet, dosed under fasted conditions in healthy subjects. Excretion of navtemadlin and the glucuronide metabolite in the urine was negligible.

Although the intrasubject variability in navtemadlin PK was <30% for the reference formulation (new tablet under fasted condition), navtemadlin PK parameters were highly variable between healthy subjects (intersubject variability), with an $AUC_{0\text{-}24}$ %CV of 55% and a C_{max} %CV of 66% after administration of the new tablet in fasted condition. Several subjects had higher exposure after each treatment, relative to most other subjects, with the maximum individual observed $AUC_{0\text{-}24}$ of ≈2 to 3 times the mean value in each cohort.

PK evidence of EHR of navtemadlin was observed as a second distinct peak around 10 hours after dosing in the concentration-time profiles of both navtemadlin and M1. This hypothesis is consistent with biliary excretion and subsequent intestinal hydrolysis of M1,

Table 4. Mean (%CV) Serum Pharmacokinetic Parameters of MIC-1 Following Administration of 60-mg Navtemadlin New (Treatment A[a]) and Old (Treatment C) Tablet Under Fasted Conditions and the New Tablet Under Fed Conditions (Treatment B)

	Treatment		
MIC-1 PD Parameter	A: 60 mg Navtemadlin New Tablet Fasted[a] N = 30	B: 60 mg Navtemadlin New Tablet Fed N = 30	C: 60 mg Navtemadlin Old Tablet Fasted N = 30
		Mean (%CV); n	
$\%CFB_{C24}$, %	2297 (101); 60	1778 (115.5); 30	139 (61.8); 30
$\%CFB_{Cmax}$, %	3759 (103.5); 60	2684 (115.7); 30	393 (62.5); 30
$AUC_{0\text{-}t}$, pg • h/mL	89409 (48.7); 60	81332 (54.2); 30	91175 (38.5); 30
$AUC_{0\text{-}24}$, pg • h/mL	32743 (49.4); 60	29820 (52.7); 30	34365 (53.4); 30
$AUC_{0\text{-}inf}$, pg • h/mL	96215 (51.9); 31	67607 (35.1); 16	110915 (30.5); 4
C_{24}, pg/mL	1318 (50.5); 60	1209 (47.7); 30	1144 (38.4); 30
C_{max}, pg/mL	2115 (56.3); 60	1819 (51); 30	2480 (66.3); 30
$Fold_{C24}$	24.0 (96.8); 60	18.8 (109.4); 30	2.39 (36); 30
$Fold_{Cmax}$	38.6 (100.9); 60	27.8 (111.5); 30	4.93 (49.8); 30
P, pg/mL	170 (119.8); 60	214 (133.2); 30	505 (41); 30
t_{max},[b] h	12.0 (8.0 – 48.0); 60	8.1 (4.0 - 36.1); 30	8.1 (4.2-36.0); 30
$t_{1/2}$,[c] h	26.5 (29.0); 31	23.5 (36.9); 16	30.6 (19.8); 4

%CFB, percent change from baseline; $\%CFB_{C24}$, percent change from predose (baseline: P) concentration at 24 hours after dosing, calculated as $([C_{24}\text{-}P]/P)*100$; $\%CFB_{Cmax}$, percent change from predose (baseline) concentration at t_{max}, calculated as $([C_{max}\text{-}P]/P)*100$; AUC_{inf}, area under the serum MIC-1 concentration–time curve from time 0 to infinity; $AUC_{0\text{-}24}$, area under the serum MIC-1 concentration-time curve from time 0 to 24 hours; $AUC_{0\text{-}t}$, area under the serum MIC-1 concentration-time curve from time 0 to time t; C_{max}, maximum observed serum MIC-1 concentration; CV, coefficient of variation; $Fold_{C24}$, fold-change in concentration from predose (baseline) at 24 hours post-dose, calculated as C_{24}/P; $Fold_{Cmax}$, fold-change in concentration from predose (baseline) at T_{max}, calculated as C_{max}/P; P, baseline predose MIC-1 concentration; PD, pharmacodynamic; $t_{1/2}$, terminal elimination half-life; t_{max}, time to C_{max}.

Treatment C Was dosed in the first period, and treatments A and B were crossed over in subsequent periods 2-4.

[a] Treatment A only: mean of 2 separate PD parameter determinations = Treatment A was administered on 2 occasions.

[b] Median (min-max); n.

[c] Arithmetic mean (%CV).

N = number of subjects per group; n = number of observations.

followed by EHR of released navtemadlin. Physiologically based PK modeling indicated that navtemadlin has a fraction absorbed that is near 100%, with absorption primarily in the duodenum and jejunum.[26] The EHR hypothesis is also consistent with ^{14}C absorption, distribution, metabolism, and excretion studies conducted in rats. In rat bile, the acyl glucuronide accounts for most of the excreted biliary radioactivity[17]; however, the glucuronide is not present in rat feces due to hydrolysis in the intestine. Similarly, urine was a minor excretion route in cynomolgus macaques. A second peak in PK profiles of both rat and monkey also indicated EHR.[17]

Navtemadlin has pH-dependent solubility that increases with increasing pH, and gastric pH could hypothetically have an effect on the PK of a weak acid such as navtemadlin.[27] *H. pylori* infection, which can increase stomach pH in a subset of infected individuals,[23,25] did not have any discernable impact on dissolution and absorption of navtemadlin. Physiologically-based PK modeling using data from the current study indicated that higher gastric pH that would occur with proton pump inhibitor administration would not increase navtemadlin exposure. Therefore, it was not surprising that the rate and extent of exposure to navtemadlin and M1 were not markedly affected in *H. pylori*–positive subjects, relative to *H. pylori*–negative subjects.

Although poor metabolizer status is generally associated with impaired glucuronidation,[28] navtemadlin and M1 exposure in heterozygous *UGT1A1*28* poor metabolizers (6/7 TA repeats, n = 16) was generally comparable to the exposure in subjects with WT *UGT1A1*28* (6/6 TA repeats, n = 12). These findings from a relatively small number of subjects indicate that *UGT1A1*28* is not likely to be rate limiting in clearance of navtemadlin. Data from a larger sample of homozygous *UGT1A1*28* poor metabolizers (7/7 TA repeats) are needed to strengthen this conclusion.

MIC-1 concentrations in serum were variable and followed the navtemadlin PK time course with a median t_{max} lag of ≈8 to 12 hours. All 3 treatment groups had generally comparable MIC-1 AUC and C_{max}, indicating that the tablet drug load or fed vs fasted administration did not meaningfully affect the PD of navtemadlin. The 60-mg navtemadlin dose elicited a reproducible and

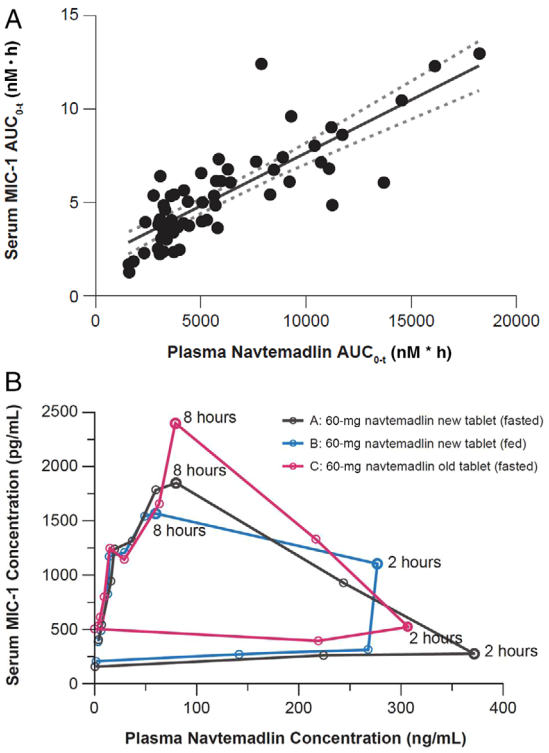

Figure 4. (A) Relationship between plasma navtemadlin concentrations and serum MIC-1 response following administration of navtemadlin new tablet under fasted conditions. Correlation plot of $AUC_{0\text{-}t}$ in nM • h units comparing navtemadlin and MIC-1 AUC (R^2 = 0.68; intercept, 1.97; slope = 0.0006). (B) Counterclockwise hysteresis in plots of the temporal relationship between MIC-1 serum concentrations and navtemadlin plasma concentrations over time that arises from the 8- to 12-h delay in serum MIC-1 t_{max}, relative to navtemadlin t_{max}. $AUC_{0\text{-}t}$, area under the plasma concentration–time curve from time 0 to the last quantifiable concentration; MIC-1, macrophage inhibitory cytokine-1; t_{max}, time to maximum concentration.

robust MIC-1 response that correlated with navtemadlin exposure, indicating concentration-dependent inhibition of the MDM2-p53 interaction and activation of p53-mediated gene transcription pathways.

The baseline MIC-1 concentration was >2-fold higher for the old tablet under fasted conditions, compared with the new tablet under fasted and fed conditions. This may be because the old tablet was administered on the first day of the 4-period study. A first-period effect may therefore have rendered first-dose PD parameters of the old tablet group (predose concentration, $Fold_{Cmax}$, $Fold_{C24}$, CFB_{Cmax}, and $\%CFB_{C24}$) different from the subsequent dose groups, despite the 1-week washout between navtemadlin doses.

In healthy subjects following administration of 60-mg navtemadlin, the pharmacodynamic half-life of MIC-1 serum elevations was >20 hours. This is consistent with observations from early clinical studies showing a stronger induction of MIC-1 in patients with cancer after repeated dosing vs single-dose administration of navtemadlin.[16] The maximal induction of MIC-1 as a PD marker of p53 activation had remarkable fidelity to the navtemadlin concentration-time profile, with similar clearance kinetics following its delayed induction.

Overall, the magnitude of MIC-1 induction appears to be dependent on both the navtemadlin dose level and the intrinsic baseline predose serum MIC-1 concentration in cancer patients.[16] In this report, healthy subjects who were administered repeated single 60-mg doses of navtemadlin had greater MIC-1 fold excursions in treatment periods when predose baseline MIC-1 serum levels were lower, confirming the observations derived from steady-state MIC-1 C_{max} levels observed with navtemadlin in the oncology treatment setting. These results, taken together, suggest that the magnitude of MIC-1 induction may not be precisely comparable across different patient populations.

Conclusions

To the best of our knowledge, this is the first account of MDM2 inhibitor pharmacokinetics and resultant MIC-1 PD in healthy subjects. The study demonstrates that a single navtemadlin dose of 60 mg, given 4 times at weekly intervals, was safe in healthy subjects. A change from the old tablet formulation to the new, film-coated, higher drug-load tablet did not markedly affect the PK of navtemadlin or the navtemadlin acyl glucuronide metabolite. A high-fat, high-calorie meal did not markedly alter navtemadlin PK, suggesting that navtemadlin can be administered without regard to food. The 60-mg dose elicited reproducible and robust MIC-1 responses, with t_{max} of 8 to 12 hours, after each navtemadlin treatment. PD MIC-1 induction was correlated with navtemadlin exposure and demonstrated concentration-dependent MDM2 target engagement in healthy subjects.

Acknowledgments

The authors thank Igor Rubets, PhD, for his contributions to the statistical design and analysis of the pharmacokinetics results for this study. This analysis was funded by Kartos Therapeutics, Inc., Redwood City, California. Medical writing and editorial assistance were provided by Swati Ghatpande, PhD, of Team 9 Science, LLC, funded by Kartos Therapeutics, Inc.

Funding

This analysis was funded by Kartos Therapeutics, Inc., Redwood City, California. Medical writing and editorial

assistance were provided by Team 9 Science, LLC, funded by Kartos Therapeutics, Inc.

Conflicts of Interest

S.W., C.K., D.L., A.H., and J.G.S. are employees of Kartos Therapeutics. J.G.S. has equity ownership with AstraZeneca. C.K. has equity ownership with AstraZeneca and Seattle Genetics. E.S. and X.W. are employees of Certara Strategic Consulting. M.A. was an employee of Certara Strategic Consulting at the time this study was conducted and is now employed at Telios Pharmaceuticals, Inc. T.P. is an employee of IV/PO: Increased Value Pharmaceutical Outsourcing, LLC. T.O. is an employee of Celerion.

References

1. Canon J, Osgood T, Olson SH, et al. The MDM2 inhibitor AMG 232 demonstrates robust antitumor efficacy and potentiates the activity of p53-inducing cytotoxic agents. *Mol Cancer Ther*. 2015;14(3):649-658.
2. Shattuck-Brandt RL, Chen SC, Murray E, et al. Metastatic melanoma patient-derived xenografts respond to MDM2 inhibition as a single agent or in combination with BRAF/MEK inhibition. *Clin Cancer Res*. 2020;26(14):3803-3818.
3. Gluck WL, Gounder MM, Frank R, et al. Phase 1 study of the MDM2 inhibitor AMG 232 in patients with advanced P53 wild-type solid tumors or multiple myeloma. *Invest New Drugs*. 2020;38(3):831-843.
4. Erba HP, Becker PS, Shami PJ, et al. Phase 1b study of the MDM2 inhibitor AMG 232 with or without trametinib in relapsed/refractory acute myeloid leukemia. *Blood Adv*. 2019;3(13):1939-1949.
5. Wong MKK, Kelly CM, Burgess MA, et al. KRT-232, a first-in-class, murine double minute 2 inhibitor (MDM2i), for TP53 wild-type (p53WT) Merkel cell carcinoma (MCC) after anti–PD-1/L1 immunotherapy. *J Clin Oncol.* 2020;38(15_suppl):10072.
6. Al-Ali HK, Delgado RG, Lange A, et al. KRT-232, a first-in-class, murine double minute 2 inhibitor (MDM2), for myelofibrosis (MF) relapsed or refractory (R/R) to Janus-associated kinase inhibitor (JAKI) treatment (tx). *HemaSphere*. 2020;4:S1, Abstract S215.
7. Verstovsek S, Al-Ali HK, Mascarenhas J, et al. BOREAS: A global phase 3 study of KRT-232, a first-in-class murine double minute 2 (MDM2) inhibitor in TP53WT relapsed/refractory (R/R) myelofibrosis (MF). *J Clin Oncol.* 2021;39(15_suppl): TPS7057.
8. An open-label, multicenter, phase 1b/2 study of the safety and efficacy of KRT-232 combined with a tyrosine kinase inhibitor (TKI) in patients with relapsed or refractory Ph+ chronic myeloid leukemia (CML). ClinicalTrials.gov Identifier: NCT04835584. https://www.clinicaltrials.gov/ct2/show/NCT04835584. Accessed May 15, 2021.
9. An open-label, multicenter, phase 1b/2 study of the safety and efficacy of KRT-232 combined with low-dose cytarabine (LDAC) or decitabine in patients with acute myeloid leukemia (AML). ClinicalTrials.gov Identifier: NCT04113616. https://clinicaltrials.gov/ct2/show/NCT04113616. Accessed August 13, 2021.
10. Hillmen P, Qamoos H, Uyei A, et al. A phase 1b-2 study of KRT-232, a first-in-class, oral, small molecule inhibitor of murine double minute 2 (MDM2), in combination with acalabrutinib for the treatment of relapsed/refractory (R/R) chronic lymphocytic leukemia (CLL) or R/R diffuse large B-cell lymphoma (DLBCL). *Blood*. 2020;136(suppl 1):23-24.
11. Mascarenhas J, Vannucchi AM, Mead AJ, et al. An open-label, global, multicenter, phase 1b/2 study of KRT-232, a first-in-class, oral small-molecule inhibitor of murine double minute 2 (MDM2), combined with ruxolitinib in patients who have myelofibrosis and a suboptimal response to ruxolitinib. *Blood* 2020;136(suppl 1):44-45.
12. KRT-232 in combination with TL-895 for the treatment of R/R MF and KRT-232 for the treatment of JAKi intolerant MF. ClinicalTrials.gov Identifier: NCT04640532. https://clinicaltrials.gov/ct2/show/NCT04640532. Accessed August 13, 2021.
13. Study of KRT-232 or TL-895 in Janus-associated kinase inhibitor treatment-naïve myelofibrosis. ClinicalTrials.gov Identifier: NCT04878003. https://clinicaltrials.gov/ct2/show/NCT04878003. Accessed August 13, 2021.
14. Tan M, Wang Y, Guan K, et al. PTGF-beta, a type beta transforming growth factor (TGF-beta) superfamily member, is a p53 target gene that inhibits tumor cell growth via TGF-beta signaling pathway. *Proc Natl Acad Sci U S A*. 2000;97(1):109-114.
15. Wischhusen J, Melero I, Fridman WH. Growth/differentiation factor-15 (GDF-15): from biomarker to novel targetable immune checkpoint. *Front Immunol*. 2020;11951. 11:951.
16. Allard M, Wada DR, Krejsa CM, Slatter JG. Exposure–macrophage inhibitory cytokine-1 (MIC-1) response analysis of the MDM2 antagonist KRT-232 in patients with advanced solid tumors, multiple myeloma, or acute myeloid leukemia. *HemaSphere*. 2020;4:S1, Abstract EP519.
17. Ye Q, Jiang M, Huang WT, et al. Pharmacokinetics and metabolism of AMG 232, a novel orally bioavailable inhibitor of the MDM2-p53 interaction, in rats, dogs and monkeys: in vitro–in vivo correlation. *Xenobiotica*. 2015;45(8):681-692.
18. Sun D, Li Z, Rew Y, et al. Discovery of AMG 232, a potent, selective, and orally bioavailable MDM2-p53

inhibitor in clinical development. *J Med Chem*. 2014;57(4):1454-1472.
19. Taylor A, Lee D, Allard M, et al. Phase 1 concentration-QTc and cardiac safety analysis of the MDM2 antagonist KRT-232 in patients with advanced solid tumors, multiple myeloma, or acute myeloid leukemia. *Clin Pharmacol Drug Dev*. 2021;10(8):918-926.
20. Ma SC, Wada R, Allard M, et al. Population pharmacokinetic analysis of the MDM2 inhibitor KRT-232 (formerly AMG 232) in subjects with advanced solid tumors, multiple myeloma or acute myeloid leukemia. *Blood*. 2019;134(suppl_1):5766-.
21. Deng J, Zhu X, Chen Z, et al. A review of food-drug interactions on oral drug absorption. *Drugs*. 2017;77(17):1833-1855.
22. El-Omar EM. Mechanisms of increased acid secretion after eradication of *Helicobacter pylori* infection. *Gut*. 2006;55(2):144-146.
23. Lahner E, Virili C, Santaguida MG, et al. *Helicobacter pylori* infection and drugs malabsorption. *World J Gastroenterol*. 2014;20(30):10331-10337.
24. Takahashi S, Fujiwara Y, Nakano K, et al. Safety and pharmacokinetics of milademetan, a MDM2 inhibitor, in Japanese patients with solid tumors: a phase I study. *Cancer Sci*. 2021;112(6):2361-2370.
25. El-Omar EM, Oien K, El-Nujumi A, et al. *Helicobacter pylori* infection and chronic gastric acid hyposecretion. *Gastroenterology*. 1997;113(1):15-24.
26. Dong J, Fraczkiewicz G, Wong S, Podoll T, Slatter JG. Mechanistic absorption physiologically-based pharmacokinetic (PBPK) model for the murine double minute 2 (MDM2) inhibitor KRT-232: prediction of food and proton pump inhibitor effects. *HemaSphere*. 2021;Abstract EP1073
27. Patel D, Bertz R, Ren S, et al. A systematic review of gastric acid-reducing agent-mediated drug-drug interactions with orally administered medications. *Clin Pharmacokinet*. 2020;59(4):447-462.
28. Sanchez-Dominguez CN, Gallardo-Blanco HL, Salinas-Santander MA, et al. Uridine 5′-diphosphoglucuronosyltransferase: its role in pharmacogenomics and human disease. *Exp Ther Med*. 2018;16(1):3-11.

Supplemental Information

Additional supplemental information can be found by clicking the Supplements link in the PDF toolbar or the Supplemental Information section at the end of web-based version of this article.